J. Fluid Mech. (1985), *vol.* 156, *pp.* 463–477
Printed in Great Britain

The inertial draining of a thin fluid layer between parallel plates with a constant normal force. Part 1. Analytic solutions; inviscid and small- but finite-Reynolds-number limits

By S. WEINBAUM, C. J. LAWRENCE AND Y. KUANG
Department of Mechanical Engineering, The City College of The City University of New York, New York, New York 10031

(Received 11 October 1984 and in revised form 30 January 1985)

The draining of thin fluid layers between rigid or deformable surfaces has been extensively studied in the limit of thin films where inertial effects are of negligible importance. In the present investigation, which is in two parts, we shall examine the inertial draining of a thin fluid layer between planar parallel surfaces under the action of a constant normal force. This is a simple model for dropping a sheet of paper or a book on a table or applying a piston to a microchip. The novelty of the problem is that we shall consider both the inertia of the object and that of the fluid for all Reynolds numbers where the flow remains laminar. In Part 1 of the study we shall derive a simplified Navier–Stokes equation for the general case which contains the dynamic equation for the motion of the object. Solutions will be presented for the time-dependent motion of the object and the intervening fluid in the gap for all ratios of object to fluid inertia in the limit of infinite Reynolds number and for small Reynolds numbers ($Re < 10$) in the limit where the time rate of change of momentum of the object is small compared with that of the fluid in the gap. In Part 2, we shall examine the limit where time-dependent boundary layers develop along the top and bottom surfaces in response to the time-varying core flow and also present a new exact Navier–Stokes solution for a time-dependent double-axisymmetric stagnation-point flow.

1. Introduction

The time-dependent draining of a fluid layer between solid surfaces is a common phenomenon that occurs in such diverse applications as the spreading of a fluid layer between glass plates, the draining of squeeze films between electrically or thermally conducting surfaces, the dropping of a book or sheet of paper on a table and a wide variety of problems involving lubricating layers. The vast majority of existing analyses have been for thin fluid layers where the Reynolds number based on gap height is sufficiently small for all inertia effects to be neglected, the so-called lubrication limit. These lubrication-theory analyses have also been applied to deformable boundaries such as elastohydrodynamic squeeze films (Christensen 1962; Rohde, Whicker & Browne 1976), the draining of fluid films in suspensions when a small particle or droplet approaches a fluid–fluid interface (Hartland 1968, 1969; Jones & Wilson 1978; Dimitrov & Ivanov 1978) and the time-dependent trapping of fluid beneath a fluid-cell membrane (Wu & Weinbaum 1982). In the two present papers we shall treat what might appear to be a much simpler problem, the

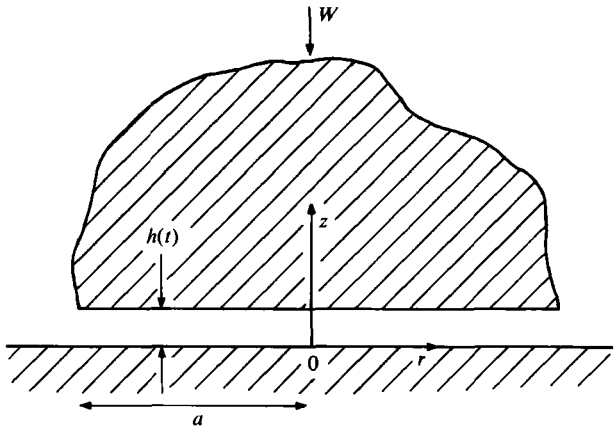

FIGURE 1. Sketch of the geometry showing the coordinate axes and dimensions.

draining of a fluid layer between two rigid parallel planar surfaces under a constant applied force such as an object falling under gravity toward a plane. The important difference is that the present analysis will consider both the inertia of the object and the inertia of the fluid in the intervening gap. For mathematical simplicity the bottom of the object will be a plane circular disk. The fluid motion in the gap can be visualized as a double time-dependent axisymmetric stagnation-point flow as shown in figure 1.

The non-dimensionalization of the governing equations for the motion of the object and of the intervening fluid shows that there are three important characteristic timescales. The viscous diffusion timescale is $t_d = h_0^2/\nu$, where h_0 is the initial gap height and ν is the kinematic viscosity of the fluid. The inertial timescale is $t_i = (\pi\rho a^4/4W)^{\frac{1}{2}}$, where ρ is the density of the fluid, a is the radius of the disk and W is the net force acting on the object when the system is at rest: $W = (m - m_b)g + F$ where m is the mass of the object, m_b is the mass of fluid displaced by the object and F is the external force. The third timescale is $t_g = (mh_0/W)^{\frac{1}{2}}$; when there is no external force and buoyancy is negligible, $W = mg$ and t_g reduces to $(h_0/g)^{\frac{1}{2}}$, which is the gravitational timescale for an object falling a distance h_0 in a vacuum. The characteristic diffusion time for the viscous boundary layers on the top and bottom boundaries to spread throughout the gap is t_d, t_i is the timescale for the fluid layer to drain in the absence of viscosity and t_g characterizes the time that it would take the object to fall in the absence of hydrodynamic forces. A fourth timescale which is not independent of the others is the viscous flow time, $t_v = t_i^2/t_d = \pi\mu a^4/4Wh_0^2$. This characterizes the time for the fluid to drain in the absence of inertia. The above definition of t_i gives rise to a characteristic inertial settling velocity $V = h_0/t_i = 2(h_0/a)(W/\pi\rho a^2)^{\frac{1}{2}}$. The ratios of the three characteristic timescales define two fundamental dimensionless groups:

$$Re = \frac{t_d}{t_i} = \frac{h_0 V}{\nu}, \quad \beta = \frac{t_g^2}{t_i^2} = \frac{4h_0 m}{\pi\rho a^4}. \tag{1}$$

The first group is a Reynolds number based on the inertial settling velocity defined above and the second group is the ratio of the squares of the gravitational and inertial settling times. Since the mass of the fluid in the gap is $m_f = \pi\rho a^2 h_0$, β can also be written as $4(h_0/a)^2(M/m_f)$, which is particularly convenient for defining the regimes of motion.

In all applications we shall assume that the ratio h_0/a is sufficiently small for the

edge effects near $r = a$ to be confined to a small part of the total gap area and therefore to be unimportant in determining both the velocity and pressure distributions in the intervening fluid space. Even with this limitation, a rather surprising diversity of behaviour can be anticipated when the object is dropped from rest, determined by the relative ordering of the three basic timescales as expressed in the magnitudes of the dimensionless numbers β and Re just defined. For a small piston applied to a microchip, Re is of the order of 0.1, whereas for a book released 1 cm above a desk top Re is of the order of 10^3 to 10^4. The physically realizable range of β depends strongly on the working fluid. For a liquid m/m_f is typically of the order of 1 to 10 and therefore, if $h_0/a < 0.1$, β will be small compared to unity in most situations. On the other hand, for air typical values of this mass ratio will be 10^3 or larger. For a sheet of paper dropped from a height of 1 cm, β will be of order unity, whereas, for a pane of glass or a book dropped from this height, β will be of the order of 10^2.

The foregoing estimates are intended to provide some feeling for the regimes of behaviour. When $t_g \gg t_i$ or $\beta \gg 1$, the primary force balance is between the net force on the object and its rate of change of momentum. The velocities and accelerations in the fluid gap will not be sufficient to generate a significant hydrodynamic pressure on the underside of the object, and it will fall almost as if it were in a vacuum. In the other limit $t_g \ll t_i$ or $\beta \ll 1$, the net weight of the object is instantly supported almost entirely by the hydrodynamic pressure on its underside with the result that the object experiences very small accelerations compared with gravity. The contrast is easily illustrated by dropping a book and a piece of paper on a table, where only the latter exhibits a slow, hovering descent.

It will be shown that, even when the full nonlinear inertia terms are retained in the governing equations for the fluid motion in the gap, the velocity field assumes a particularly simple radial dependence for all Reynolds numbers with the result that the pressure field, while not constant across the fluid layer as in lubrication or boundary-layer theory, is still a relatively simple quadratic function of r. This simplification will make it possible to develop analytic solutions in various limits and, for the small-β case, present a new time-dependent exact numerical solution to the full Navier–Stokes equations. In this first paper, we shall give the general formulation and develop analytic solutions for the inviscid limit for all values of β and also for low- but finite-Reynolds-number flows for small values of β. In the second paper we shall present a new exact numerical solution to the simplified set of Navier–Stokes equations valid for all Reynolds numbers in the limit of small β and an approximate high-Reynolds-number solution which is valid until the boundary layers on the top and bottom surfaces merge. The new numerical solution is exact in the same sense as the axisymmetric-stagnation-point-flow problem (Homann 1936) or the rotating-disk problem (von Kármán 1921), in that the radial dependence can be factored out of the governing differential equations before they are numerically integrated.

The diversity of limiting cases, the presence of time-dependent boundary layers, the relatively simple analytic solutions and the availability of exact numerical solutions make the problem an excellent one for illustrative pedagogical purposes. In fact, the problem was introduced by the first author in a graduate course in viscous flow because of the diversity of physical behaviour illustrated by the limiting cases even before its simplifying mathematical features were fully realized.

2. General formulation

As shown in figure 1, it is convenient to illustrate the problem as a disk of arbitrary thickness released from rest and falling toward a solid planar surface. The fluid gap is independent of r and varies only with time. Geometrical dimensions and coordinate axes are as shown in the figure.

Because of the axial symmetry of the flow and the nature of the velocity boundary conditions, it is evident that a stream function of the form

$$\psi = r^2 F(z,t), \tag{2}$$

where

$$u = rF_z(z,t), \quad w = -2F(z,t), \tag{3}$$

will be sufficiently general to satisfy both the continuity equation and the viscous-flow conditions at both $z = 0$ and $z = h(t)$ for all t. These boundary conditions are

$$F = 0, \qquad F_z = 0 \quad \text{on} \quad z = 0, \tag{4a,b}$$

$$F = -\tfrac{1}{2}h_t, \quad F_z = 0 \quad \text{on} \quad z = h(t), \tag{5a,b}$$

where h_t is the instantaneous velocity of the disk. The initial conditions are

$$F = 0, \quad h = h_0, \quad h_t = 0 \quad \text{when} \quad t=0. \tag{6a,b,c}$$

Substituting (2) and (3) into the Navier–Stokes equation, one obtains for the radial and axial components

$$rF_{zt} + rF_z^2 - 2rFF_{zz} - \nu rF_{zzz} = -\frac{1}{\rho}p_r, \tag{7}$$

$$-2F_t + 4FF_z + 2\nu F_{zz} = -\frac{1}{\rho}p_z. \tag{8}$$

It can be seen that the r dependence can be factored out of the left-hand side of (7) and an unknown function $A(z,t)$ can be defined by

$$A(z,t) = \nu F_{zzz} + 2FF_{zz} - F_z^2 - F_{zt}. \tag{9}$$

Substituting this definition of $A(z,t)$ into (7) and integrating over r, one obtains the following form for the pressure

$$p(r,z,t) = \tfrac{1}{2}\rho r^2 A(z,t) + B(z,t), \tag{10}$$

where $B(z,t)$ is an unknown function resulting from the integration.

Equation (10) is now differentiated with respect to z and the result used in (8),

$$\tfrac{1}{2}\rho r^2 A_z + B_z = -2\rho(\nu F_{zz} - F_t + 2FF_z). \tag{11}$$

Since the right-hand side of (11) is independent of r, it follows that

$$A_z = 0, \quad \text{so} \quad A(z,t) = A(t), \tag{12}$$

and

$$B_z = -2\rho(\nu F_{zz} - F_t + 2FF_z). \tag{13}$$

It is evident from (10) that $B(h,t)$ is simply the pressure $p_0(t)$ at the centre $r = 0$ of the lower surface of the body. Thus from (10) and (12), the pressure distribution on this surface is

$$p(r,h,t) = \tfrac{1}{2}\rho r^2 A(t) + p_0(t). \tag{14}$$

The unknown function $A(t)$ can be related to the instantaneous acceleration of the disk through a macroscopic force balance

$$mh_{tt} = -W + D(t), \tag{15}$$

where

$$W = (m - m_b)g + F \tag{16}$$

and $D(t)$ is the hydrodynamic force on the disk. An exact description of $D(t)$ would require knowledge of the complete geometry of the object and the velocities and accelerations everywhere. In effect one would need to know the instantaneous virtual mass and Basset force on the disk as determined by the entire geometry including the planar surface $z = 0$. It is clear, however, that, if $h_0 \ll a$, the velocities and accelerations within the fluid gap will be much larger than in the rest of the flow field, with the result that the major portion of the hydrodynamic force on the disk will be due to fluid motion in the gap, both viscous and inertial forces being considered. The viscous stresses do not contribute to the normal force on the disk and thus $D(t)$ will be given by the approximation

$$D(t) = \int_0^a 2\pi r p(r, h, t)\,\mathrm{d}r = \tfrac{1}{4}\pi\rho a^4 A(t) + \pi a^2 p_0(t). \tag{17}$$

Since the buoyancy force due to hydrostatic pressure variation has already been considered in (16), $p_0(t)$ is measured relative to a dynamic reference pressure at the edge of the disk, which may be treated as zero if the small drop in pressure across the exit expansion is neglected. This approximation is accurate to $O(h_0/a)$. One concludes from (14) that

$$p_0(t) = -\tfrac{1}{2}\rho a^2 A(t), \tag{18}$$

and therefore that $D(t)$ from (17) is approximately

$$D(t) = -\tfrac{1}{4}\pi\rho a^4 A(t). \tag{19}$$

Substituting (19) into (15), solving for $A(t)$ and inserting the result in (9), one obtains

$$\nu F_{zzz} + 2FF_{zz} - F_z^2 - F_{zt} = -\frac{4}{\pi\rho a^4}(mh_{tt} + W). \tag{20}$$

The original boundary-value problem has thus been reduced to the solution of (20) subject to boundary and initial conditions (4)–(6). Equation (5*a*) provides an independent relation coupling F and h.

The pressure field in the gap is obtained by integrating (13), substituting this result in (10) and using (18). This leads to the expression

$$p(r, z, t) = \tfrac{1}{2}\rho A(t)(r^2 - a^2) - 2\rho\left(\nu F_z + F^2 - \tfrac{1}{4}h_t^2 + \int_z^h F_t\,\mathrm{d}z\right). \tag{21}$$

The second group of terms on the right-hand side of (21) vanishes at $z = h(t)$ with the result that the pressure distribution on the underside of the object is always parabolic with maximum pressure $p_0(t)$, which from (15), (18) and (19) is given by

$$p_0(t) = \frac{2}{\pi a^2}(mh_{tt} + W) = -\tfrac{1}{2}\rho a^2 A(t). \tag{22}$$

From (21) the radial pressure gradient is constant across the gap, but the pressure varies with z as given by the second group of terms involving F and its derivatives. It is in this property that the pressure field in the present problem differs from both standard boundary-layer theory and thin-film-lubrication theory.

To cast (20) in non-dimensional form, we need a lengthscale for z and $h(t)$, a velocity scale for F and a characteristic timescale t_c, which for the moment we shall leave unspecified. We thus define $z^* = z/h_0$, $h^* = h/h_0$, $F^* = F/(h_0/t_c)$ and $t^* = t/t_c$.

Substituting these dimensionless variables in (20) and dropping the asterisks for convenience, one obtains

$$F_{zt} + F_z^2 - 2FF_{zz} - \frac{t_c}{t_i}\frac{1}{Re}F_{zzz} = \beta h_{tt} + \frac{t_c^2}{t_i^2}, \tag{23}$$

where Re and β are defined in (1) and t_i is given by

$$t_i = \left(\frac{\pi\rho a^4}{4W}\right)^{\frac{1}{2}}. \tag{24}$$

The choice of t_c depends on the timescale of interest. The most obvious choice is to use t_i, but we shall show that interesting behaviour occurs on other timescales. In the rest of this paper we shall look into the behaviour of the solution to (23) in the limit of infinite Re and in the limit of zero β with small but finite Re.

3. Inviscid (infinite Re) limit

In the infinite Re limit, the boundary layers at $z = 0$ and $z = h$ are assumed to be vanishingly thin and thus the viscous term in (23) is negligible throughout the gap. The high- but finite-Re case will be treated in Part 2 (Lawrence, Kuang & Weinbaum 1985). For the weight and fluid inertia forces to be of the same order, we require that $t_c = t_i$. Equation (23) then reduces to

$$F_{zt} + F_z^2 - 2FF_{zz} = \beta h_{tt} + 1. \tag{25}$$

The fluid motion in the gap has the form of a time-dependent inviscid axisymmetric stagnation-point flow, where u is independent of z and increases linearly with r. The stream function ψ in (2) takes the simplified form $\psi = r^2 z\phi(t)$. Then $F^* = z^*\phi^*(t^*)$, where $\phi^* = \phi t_c$, and, after dropping the asterisks, (25) reduces to

$$\phi_t + \phi^2 = \beta h_{tt} + 1. \tag{26}$$

Boundary condition (5a) becomes

$$2\phi h = -h_t. \tag{27}$$

Equation (27) can be used to eliminate ϕ and its derivatives from (25). The resulting equation is

$$\left(\beta + \frac{1}{2h}\right)h_{tt} - \frac{3}{4h^2}h_t^2 + 1 = 0. \tag{28}$$

The initial conditions for (28) are $h = 1$ and $h_t = 0$.

Equation (28) is a nonlinear ordinary differential equation which has to be solved numerically in the general case. Useful asymptotic solutions can be obtained for three limiting cases: (a) $\beta \ll 1$ all h; (b) $h \approx 1$ all β; (c) $\beta \gg 1$ all h. It will be convenient to write (26) and (27) so that derivatives of h do not appear. Equation (27) can be re-written

$$-h_{tt} = 2h\phi_t + 2\phi h_t = 2h(\phi_t - 2\phi^2). \tag{29}$$

Substituting this result in (26) and regrouping terms, one has

$$\phi_t(1 + 2\beta h) + \phi^2(1 - 4\beta h) = 1. \tag{30}$$

It is evident that: (i) if $\beta = 0$, (30) simplifies for all $h \leqslant 1$ to

$$\phi_t + \phi^2 = 1, \tag{31}$$

and (ii) for $h \approx 1$ (short times) and all β, (30) is approximated by

$$\phi_t + B\phi^2 = C, \tag{32}$$

where $$B = \frac{1-4\beta}{1+2\beta}, \quad C = \frac{1}{1+2\beta}.$$

(*a*) *Solution $\beta \to 0$ limit*

The solution of (31) subject to the initial condition $\phi = 0$ is

$$\phi(t) = \tanh t. \tag{33}$$

Substituting this result in (27) and integrating with initial condition $h = 1$, one obtains

$$h(t) = \frac{1}{\cosh^2 t}. \tag{34}$$

The instantaneous velocity of the disk is

$$h_t = -2\frac{\tanh t}{\cosh^2 t}. \tag{35}$$

The solutions for small β, (33) and (34), describe the limit where the rate of change of momentum of the disk is negligible and the hydrodynamic pressure instantly supports its weight. From the definition of β, the inertial contribution to the force balance of the fluid in the gap is much larger than that of the disk itself.

(*b*) *Short-time solution ($h \approx 1$) for all β*

At very early times when the disk is near to its original position, $h = 1$, the motion is governed by (32). The solution of (32) is of similar form to case (*a*), $\beta \ll 1$, except that the constant B vanishes when $\beta = \frac{1}{4}$, with the result that separate solutions have to be obtained for $\beta < \frac{1}{4}$, $\beta > \frac{1}{4}$ and $\beta = \frac{1}{4}$. The solution for $\beta < \frac{1}{4}$ is

$$\phi(t) = \left(\frac{C}{B}\right)^{\frac{1}{2}} \tanh\left[(BC)^{\frac{1}{2}}t\right], \tag{36}$$

$$h(t) = \cosh^{-2/B}\left[(BC)^{\frac{1}{2}}t\right]. \tag{37}$$

In the limit where $\beta \ll 1$, $B = C = 1$ and results (36) and (37) reduce to (34) and (35). This may seem surprising since (32) is only valid near $h = 1$, whereas results (34) and (35) are valid for all h. The explanation lies in the fact that the neglected β terms in (30) which have been approximated near $h = 1$ in writing (32) are always small if $\beta \ll 1$.

To find a solution for $\beta > \frac{1}{4}$, we define a new positive constant

$$D = -B = \frac{4\beta-1}{1+2\beta},$$

and rewrite equation (32) as

$$\phi_t - D\phi^2 = C. \tag{38}$$

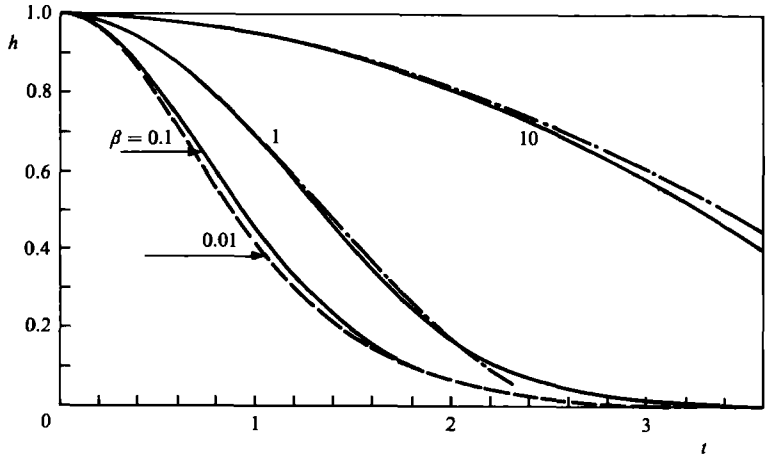

FIGURE 2. Time dependence of h in the inviscid limit (timescale based on t_i): ——, exact numerical solution, (28); –·–·–, approximate solution for $h \approx 1$, (37) and (40); – – – –, analytic solution for small β, (34).

The solutions of (38) and (27) are

$$\phi(t) = \left(\frac{C}{D}\right)^{\frac{1}{2}} \tan\left[(CD)^{\frac{1}{2}} t\right], \tag{39}$$

$$h(t) = \cos^{2/D}\left[(CD)^{\frac{1}{2}} t\right]. \tag{40}$$

For $\beta = \frac{1}{4}$, (32) or (38) is linear and has the simple solution

$$\phi(t) = \tfrac{2}{3}t, \tag{41}$$

and, from (27),

$$h(t) = \mathrm{e}^{-\frac{2}{3}t^2}. \tag{42}$$

(c) *Large-β solution*

The limiting case $\beta \gg 1$ corresponds to the rate of change of momentum of the disk being much larger than the hydrodynamic forces. The disk falls almost as if it were in a vacuum with

$$h(t) = 1 - \frac{t^2}{2\beta}. \tag{43}$$

4. Results and discussion of the inviscid limit

In figure 2 we have plotted the solutions for the instantaneous position of the disk in the inviscid limit. For $\beta = 0.01$ the $\beta = 0$ analytic solution is indistinguishable from the numerical solution or the $h \approx 1$ approximation and only a single curve is shown. As explained previously the $h \approx 1$ approximation is actually valid for all h when $\beta \ll 1$ since (30) reduces to (31). For $\beta < \frac{1}{4}$ (37) provides a reasonable approximation for all times whereas for $\beta > \frac{1}{4}$ the large-time behaviour of (40) is more subtle. Inspection of (30) shows that provided $\beta h \gg 1$ (30) can be approximately represented by $\phi_t - 2\phi^2 = 0$. The solution for ϕ thus behaves as if it were independent of h provided $h \gg 1/\beta$. Equation (38) and solution (40) are therefore valid except for small values of h of order $1/\beta$ when $\beta \gg 1$. This behaviour corresponds to an object falling over most of the initial height h_0 as if it were in a vacuum until a thin layer of fluid is left before contact at which time hydrodynamic forces become important.

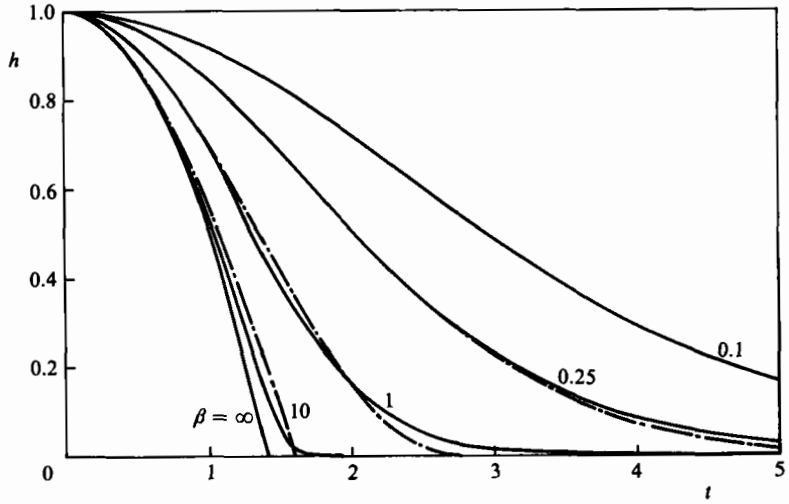

FIGURE 3. Time dependence of h in the inviscid limit (timescale based on t_g): ——, exact numerical solution, (28); –·–·–, approximate solution for $h \approx 1$, (37), (40) and (42).

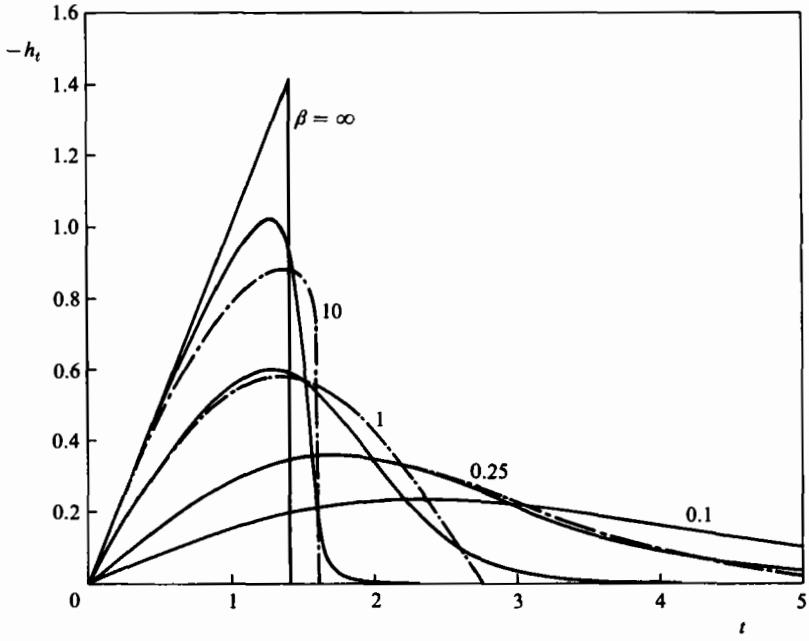

FIGURE 4. Time dependence of disk velocity in the inviscid limit (timescale based on t_g): ——, exact numerical solution, (28); –·–·–, approximate solution for $h \approx 1$, (37), (40) and (42).

The physical significance of the results is clearer if the position and velocity of the disk are plotted on the dimensionless timescale t/t_g as in figures 3 and 4. For $\beta \ll 1$ the descent of the object is arrested starting at $t = 0$ by the inertia of the fluid and the acceleration of the object is never important. The peak in the velocity results from the fact that as the gap narrows a smaller velocity of descent is required to maintain the radial velocity component and the pressure distribution on the underside of the disk. For $\beta > 1$ the object accelerates until its inertia becomes comparable to that of the fluid in the gap and the peak velocity is achieved when

the hydrodynamic and applied forces balance. For $\beta \ll 1$ this balance exists for all time since the inertia of the object is negligible. For $\beta \gg 1$, as noted above, hydrodynamic forces slow the fall of the disk only before contact.

5. Limit of small β

In many applications of this theory, the rate of change of momentum of the moving body is negligible compared to the hydrodynamic forces, so β will be small. The limiting case $\beta = 0$ is not singular even though β is the coefficient of the highest-order time derivative in (23). The initial condition (6*c*) is superfluous because it is not independent of the other initial and boundary conditions and so will always be satisfied, even if the term βh_{tt} is dropped from (23). This is demonstrated by solution (34) for the case of infinite Re and is also readily deduced from (28) where condition (5*a*) has been utilized and the coefficient of the h_{tt} term is unaffected by the limit $\beta = 0$. With this approximation, (22) reduces to $p_0(t) = (2W/\pi a^2)$, so the pressure on the underside of the body is time independent. The radial pressure gradient becomes a function of r only, and after separation of the r dependence, it is a constant.

Useful approximate solutions may be obtained in three limiting cases (*a*) $Re \ll 1$, (*b*) $h \approx 1$, (*c*) $Re \gg 1$. Case (*a*) is the extension of the classical lubrication theory with $Re = 0$ to the case of small but finite Re, and is presented below. Cases (*b*) and (*c*) will be included with the full numerical solution in Part 2 (Lawrence, Kuang & Weinbaum 1985).

The standard lubrication theory calls for a balance between the viscous and radial-pressure-gradient terms in (23). This balance is achieved if t_c is chosen to be $t_v = t_1/Re$. Introducing a new dimensionless time $T = t/t_v$ and stream function $f = Ft_v/h_0$, one obtains

$$f_{zzz} + 1 = Re^2 (f_{zT} + f_z^2 - 2ff_{zz}). \tag{44}$$

The required solution is an expansion, asymptotic for fixed t as $Re \to 0$, in the form

$$f(z, T; Re) \sim f_0(z, h(T)) + Re^2 f_2(z, h, h_T) + O(Re^4), \tag{45}$$

$$h(T; Re) \sim h_0(T) + Re^2 h_2(T) + O(Re^4). \tag{46}$$

Relation (45) is substituted into (44) and the boundary conditions (4) and (5*b*). The result of the substitution must be valid for any small Re, so that the coefficients of each power of Re^2 form independent equations.

At zero order, one obtains

$$f_{0zzz} + 1 = 0, \tag{47}$$

with boundary conditions

$$f_0 = 0, \quad f_{0z} = 0 \quad \text{on} \quad z = 0, \tag{48}$$

$$f_{0z} = 0 \quad \text{on} \quad z = h(T). \tag{49}$$

The solution of (47)–(49) gives the lubrication-theory result

$$f_0 = \tfrac{1}{4}hz^2 - \tfrac{1}{6}z^3, \tag{50}$$

which is a parabolic radial-velocity profile $u = \frac{1}{2}rz(h-z)$. At second order, one finds

$$\begin{aligned} f_{2zzz} &= f_{0zT} + f_{0z}^2 - 2f_0 f_{0zz} \\ &= \tfrac{1}{12}(6zh_T + 2z^3 h - z^4), \end{aligned} \tag{51}$$

with boundary conditions

$$f_2 = 0, \quad f_{2z} = 0 \quad \text{on} \quad z = 0, \tag{52}$$

$$f_{2z} = 0 \quad \text{on} \quad z = h(T). \tag{53}$$

Equations (51)–(53) have the solution

$$f_2 = \tfrac{1}{5040}[105h_T(z^4 - 2z^2h^2) - 2z^7 + 7z^6h - 14z^2h^5]. \tag{54}$$

Initial condition (6*a*) cannot be satisfied, showing that an 'inner' expansion will be required on a shorter timescale which must be matched to (45) and (46). This is dealt with in the next paragraph. Substituting (46), (50) and (54) into boundary condition (5*a*) and separating in powers of Re^2 one obtains two equations for h_0 and h_2:

$$h_{0T} = -\tfrac{1}{6}h_0^3, \tag{55a}$$

$$h_{2T} + \tfrac{1}{2}h_0^2 h_2 = \tfrac{1}{24}h_0^4 h_{0T} + \tfrac{18}{5040}h_0^7. \tag{55b}$$

Equation (55*a*) has the general solution

$$h_0 = \left(\frac{3}{T + C_0}\right)^{\frac{1}{2}}, \tag{56}$$

which can be used to find the general solution to (55*b*)

$$h_2 = C_1\left(\frac{3}{T + C_0}\right)^{\frac{3}{2}} + \frac{17}{1680}\left(\frac{3}{T + C_0}\right)^{\frac{5}{2}}. \tag{57}$$

The initial conditions (6*b*, *c*) cannot be used to find the constants C_0 and C_1 since the velocity profiles obtained from (50) and (54) do not satisfy the correct initial condition as mentioned above.

The appropriate timescale for the inner expansion is $t_d = Re\, t_i$. Taking this value for t_c in (23) and using τ for the dimensionless short time and G for the dimensionless inner stream function, one obtains

$$G_{z\tau} + G_z^2 - 2GG_{zz} - G_{zzz} = Re^2. \tag{58}$$

τ and G are related to T and f by $\tau = T/Re^2$, $G = Re^2 f$. The solution is required to be asymptotic for fixed τ as $Re \to 0$ and of the form

$$G(z, \tau;\, Re) \sim Re^2\, G_2(z, \tau) + O(Re^4), \tag{59}$$

$$h(\tau;\, Re) \sim 1 + Re^2\, H_2(\tau) + O(Re^4). \tag{60}$$

Relations (59) and (60) are first substituted into (58), (4) and (6). To lowest order in Re^2 one gets

$$G_{2z\tau} - G_{2zzz} = 1; \tag{61}$$

$$G_2 = 0, \quad G_{2z} = 0 \quad \text{on} \quad z = 0, \tag{62}$$

$$G_2 = 0, \quad H_2 = 0 \quad \text{when} \quad t = 0. \tag{63a, b}$$

Boundary conditions (5) are now expanded in Taylor series about $z = 1$ and the coefficients of powers of Re^2 are equated. This gives

$$G_2 = -\tfrac{1}{2}H_{2\tau}, \quad G_{2z} = 0 \quad \text{on} \quad z = 1. \tag{64a, b}$$

Equations (61), (62) and (63*a*) have a separable solution

$$G_2 = \tfrac{1}{4}z^2 - \tfrac{1}{6}z^3 - \sum_{n \text{ odd}} \frac{4}{n^4\pi^4}(1 - \cos n\pi z)\, e^{-n^2\pi^2\tau}. \tag{65}$$

Substituting (65) in (64b) and satisfying (64a) one obtains

$$H_2 = -\tfrac{1}{6}\tau + \sum_{n \text{ odd}} \frac{16}{n^6\pi^6}(1-\mathrm{e}^{-n^2\pi^2\tau}). \tag{66}$$

The two solutions (46) and (60) for h are both valid on the intermediate timescale with variable $s = Re^{2\alpha}T$ provided $0 < \alpha < 1$. The solutions are matched by expressing each in terms of the variable s and requiring that the coefficients of each power of Re^2 be equal. This gives the values

$$C_0 = 3, \quad C_1 = \tfrac{11}{1680}. \tag{67}$$

Summarizing these results, one has on the long timescale

$$h \sim (1+\tfrac{1}{3}T)^{-\frac{1}{2}} + Re^2\tfrac{1}{1680}[11(1+\tfrac{1}{3}T)^{-\frac{3}{2}} + 17(1+\tfrac{1}{3}T)^{-\frac{5}{2}}] + O(Re^4), \tag{68}$$

$$h_T \sim -\tfrac{1}{6}(1+\tfrac{1}{3}T)^{-\frac{3}{2}} - Re^2\tfrac{1}{10080}[33(1+\tfrac{1}{3}T)^{-\frac{5}{2}} + 85(1+\tfrac{1}{3}T)^{-\frac{7}{2}}] + O(Re^4). \tag{69}$$

On the short timescale $\tau = T/Re^2$,

$$h \sim 1 - Re^2\frac{1}{6}\left[\tau - \sum_{n \text{ odd}} \frac{96}{n^6\pi^6}(1-\mathrm{e}^{-n^2\pi^2\tau})\right] + O(Re^4), \tag{70}$$

$$h_\tau \sim -Re^2\frac{1}{6}\left[1 - \sum_{n \text{ odd}} \frac{96}{n^4\pi^4}\mathrm{e}^{-n^2\pi^2\tau}\right] + O(Re^4). \tag{71}$$

The long-timescale solution satisfies the initial condition on h with error $O(Re^2)$ even though the stream function does not satisfy its initial condition. This means that the long-timescale solution is valid almost from $t = 0$ for small values of Re. This is shown in figure 5, which shows the time dependence of h for different values of Re. Since the dimensionless times T and τ used above differ by a factor of Re^2, it is convenient to use the intermediate timescale $\tilde{t} = t/t_i = T/Re = \tau\, Re$ to plot the results (68)–(71), noting also that $h_T = (1/Re)\,h_{\tilde{t}}$. Figures 5 and 6 then show the results scaled with inertial time $t_i = (\pi\rho a^4/4W)^{\frac{1}{2}}$, length h_0 and inertial velocity $V = h_0/t_i$.

Figure 5 shows that the long-time expansion (68) is accurate for all time for Reynolds numbers up to unity. It gives a slight overshoot of the initial value of h by an amount $\frac{1}{60}Re^2$. For larger Reynolds numbers, the expansion (70) must be used for $\tilde{t}$ up to about 0.5 to account for the inertial resistance of the fluid to its initial acceleration. The matched expansions are quite accurate for Reynolds numbers up to 10, even though they were derived for $Re \ll 1$. This is because of the large denominator in the second term of (68) and because one only needs to use values of τ up to about $\frac{1}{2}Re$ in (70). Figure 6 shows that the matching of the expansions for body velocity (69) and (71) are less accurate than those for gap height (68) and (70) because expansion is a monotonic function of time, one increasing for short times and the other decreasing for large times, giving rise to curves with opposite slopes. One would expect the true velocity curve to have a smooth peak somewhat below the intersection of the two expansions.

In all the cases studied the initial acceleration of the object causes an acceleration of the fluid in the gap. For the inviscid limit this is an acceleration of a one-dimensional profile whereas for the low-Reynolds-number limit this is an acceleration to a quasi-steady profile that changes with Re. For early times the lowest-order solution for the radial-velocity profile obtained from the stream-function solution (65) is the same as the start-up flow in a parallel-wall channel in which a constant pressure gradient has been applied at $t = 0$. At larger times the radial-velocity profile to $O(Re^2)$

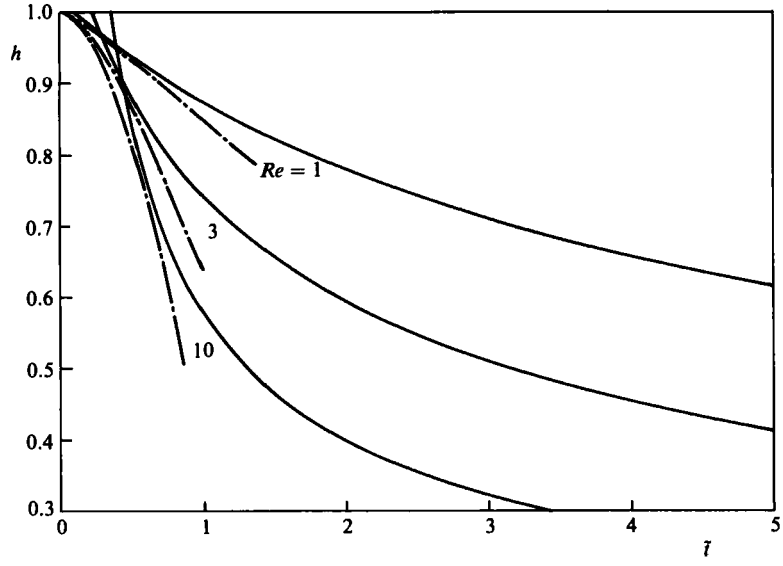

FIGURE 5. Time dependence of h for small Reynolds numbers ($\beta = 0$ limit): –·–·–, small-$\tilde{t}$ asymptotic expansion (70); ——, large-$\tilde{t}$ asymptotic expansion (68).

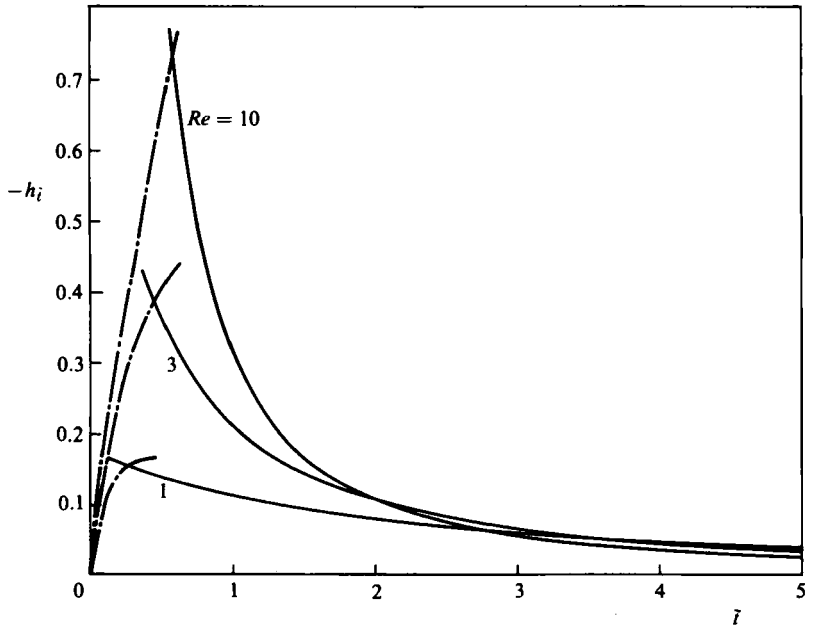

FIGURE 6. Time dependence of disk velocity for small Re ($\beta = 0$ limit): –·–·–, small-$\tilde{t}$ asymptotic expansion (71); ——, large-$\tilde{t}$ asymptotic expansion (69).

is obtained from solutions (50) and (54) and is a function of the instantaneous gap width and Re. These profiles are shown as a function of Re at fixed h in the upper half of the diagram, figure 7 (a), and as a function of h (or equivalently t) at a fixed Re in the lower half of the diagram, figure 7 (b). One observes that as either Re or h approach zero the profile becomes parabolic.

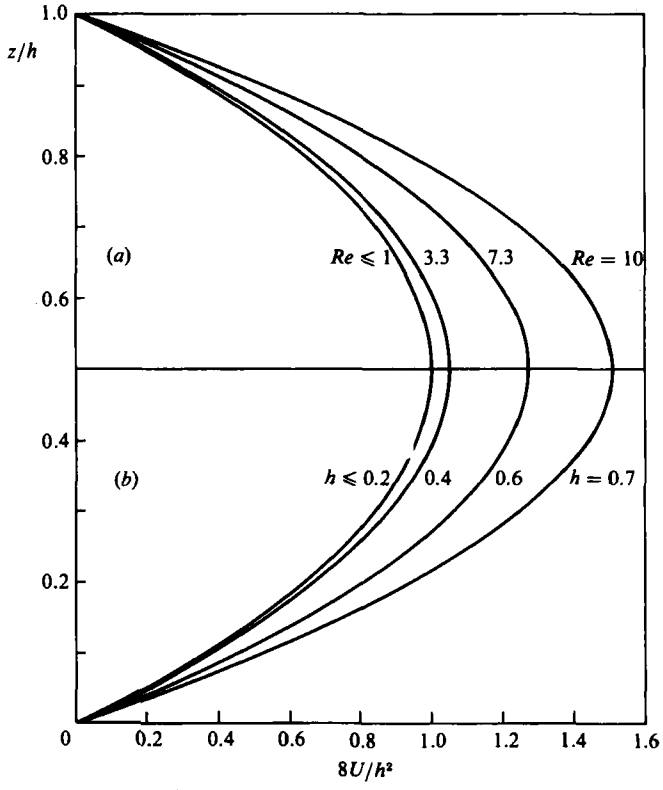

FIGURE 7. Velocity profiles in the limit $\beta = 0$ for small Re, (a) the dependence on Re at given $h = 0.7$. (b) the dependence on h for given $Re = 10$.

The long-time asymptotic decay of the motion is fundamentally different in the low-Re and the inviscid limits. In the low-Re limit the inertial terms rapidly damp out due to viscosity, and the pressure field on the underside of the disk is due to a quasi-steady pressure viscous force balance. In the inviscid limit the radial velocity, which is given by $\phi(t)r$, from (33) approaches a constant value at any r and a quasi-steady-state Bernoulli pressure distribution is established on the underside of the disk. The fascinating observation is that this pressure distribution is the same in both limits, being a simple parabolic function of r. It was this observation that suggested to the first author that a more general simplifying analysis leading to an exact numerical solution for all Re was possible. This solution and an approximate solution for the time-dependent development of the viscous boundary layers in the limit of high but finite Re are presented in Part 2 of this paper.

REFERENCES

CHRISTENSEN, H. 1962 *Proc. R. Soc. Lond.* A **266**, 312.

DIMITROV, D. S. & IVANOV, I. B. 1978 *J. Colloid Interface Sci.* **64**, 97.

HARTLAND, S. 1968 *J. Colloid Sci.* **26**, 283.

HARTLAND, S. 1969 *Chem. Engng Sci.* **24**, 987.

HOMANN, F. 1936 *Z. angew. Math. Mech.* **16**, 153.

JONES, A. F. & WILSON, S. D. R. 1978 *J. Fluid Mech.* **87**, 263.

LAWRENCE, C. J., KUANG, Y. & WEINBAUM, S. 1985 *J. Fluid Mech.* **156**, 479.
ROHDE, S. M., WHICKER, D. & BROWNE, A. L. 1976 *Trans. A.S.M.E.* F: *J. Lubric. Tech.* **98**, 401.
VON KÁRMÁN, T. 1921 *Z. angew. Math. Mech.* **1** 233.
WU, R. & WEINBAUM, S. 1982 *J. Fluid Mech.* **121**, 315.